A perpendicular graphene/ferromagnet electrode for spintronics

H. Naganuma, V. Zatko, M. Galbiati, F. Godel, A. Sander, C. Carretero, O. Bezencenet, N. Reyren, M.-B. Martin, B. Dlubak, et al.

Applied Physics Letters

A perpendicular graphene/ferromagnet electrode for spintronics

Cite as: Appl. Phys. Lett. **116**, 173101 (2020); https://doi.org/10.1063/1.5143567
Submitted: 03 January 2020 . Accepted: 09 April 2020 . Published Online: 27 April 2020

H. Naganuma, V. Zatko, M. Galbiati, F. Godel, A. Sander, C. Carrétéro, O. Bezencenet, N. Reyren, M.-B. Martin, B. Dlubak, and P. Seneor

Applied Physics Letters ARTICLE scitation.org/journal/apl

A perpendicular graphene/ferromagnet electrode for spintronics

Cite as: Appl. Phys. Lett. **116**, 173101 (2020); doi: 10.1063/1.5143567
Submitted: 3 January 2020 · Accepted: 9 April 2020 ·
Published Online: 27 April 2020

H. Naganuma,[1,2,3,4,a)] V. Zatko,[5] M. Galbiati,[5] F. Godel,[5] A. Sander,[5] C. Carrétéro,[5] O. Bezencenet,[6] N. Reyren,[5] M.-B. Martin,[5] B. Dlubak,[5,a)] and P. Seneor[5,a)]

AFFILIATIONS

[1]Center for Innovative Integrated Electronics Systems, Tohoku University, 468-1 Aoba, Aramaki, Aoba-ku, Sendai, Miyagi 980-8572, Japan
[2]Graduate School of Engineering, Tohoku University, 6-6-05 Aoba, Aramaki, Aoba-ku, Miyagi 980-8579, Japan
[3]Center for Spintronics Integrated Systems, Tohoku University, 2-2-1 Katahira, Aoba-ku, Sendai, Miyagi 980-8577, Japan
[4]Center for Spintronics Research Network, Tohoku University, 2-2-1 Katahira, Aoba-ku, Sendai, Miyagi 980-8577, Japan
[5]Unité Mixte de Physique, CNRS, Thales, Université Paris-Saclay, 91767 Palaiseau, France
[6]Thales Research and Technology, 1 Avenue Augustin Fresnel, 91767 Palaiseau, France

[a)]**Authors to whom correspondence should be addressed:** hiroshi.naganuma.c3@tohoku.ac.jp, bruno.dlubak@cnrs-thales.fr, and pierre.seneor@cnrs-thales.fr

ABSTRACT

We report on the large-scale integration of graphene layers over a FePd perpendicular magnetic anisotropy (PMA) platform, targeting further downscaling of spin circuits. An $L1_0$ FePd ordered alloy showing both high magneto-crystalline anisotropy and a low magnetic damping constant, is deposited by magnetron sputtering. The graphene layer is then grown on top of it by large-scale chemical vapor deposition. A step-by-step study, including structural and magnetic analyses by x-ray diffraction and Kerr microscopy, shows that the measured FePd properties are preserved after the graphene deposition process. This scheme provides a graphene protected perpendicular spin electrode showing resistance to oxidation, atomic flatness, stable crystallinity, and perpendicular magnetic properties. This, in turn, opens the way to the generalization of hybrid 2D-materials on optimized PMA platforms, sustaining the development of spintronics circuits based on perpendicular spin-sources as required, for instance, for perpendicular-magnetic random-access memory schemes.

Spin-based electronics are at the heart of widely distributed applications, such as sensors, read heads, and more recently magnetic random-access memories (MRAMs), which are now being steadily developed to higher densities and three-dimensional device structures.[1–3] Furthermore, spintronics is seen as one of the main contenders for post-CMOS approaches, with strong potential for spin logics[4,5] and beyond that, for instance, for stochastic calculations,[6–8] neuromorphic low power artificial intelligence,[9] and quantum computing.[10,11] These applications are promoting and sustaining the emergence of innovative spintronics material platforms to further scale spin circuits, increasing their performances and bringing next generation functionalities. In this direction, perpendicular magnetic anisotropy (PMA) materials, even if initially more complex to engineer, have appeared as a promising solution to stabilize magnetic properties, while downscaling magnetic tunnel junction (MTJ) array dimensions. This has led to the fabrication of spin devices such as perpendicular-MRAM (*p*-MRAM),[12,13] spin torque oscillators,[14] and spin diodes.[15] Interestingly, among the family of PMA materials, $L1_0$-ordered alloys such as FePd or MnGa present the double benefit of large PMA ($\sim$1 MJ/m^3) and room temperature low magnetic damping constant, foreseen to reduce the electrical consumption of spin-transfer torque magnetization switching.[15–17] Similarly, graphene has been put forward for PMA platforms as it can induce interfacial PMA, owing to orbital-hybridization with magnetic metals,[18] reminiscent of the case of MgO/CoFeB systems.[19–21] Remarkably, the association of graphene with ferromagnetic systems has been recently shown to stabilize topological spin textures as required for skyrmion-based circuits thanks to Rashba effects.[22] This can be added to the spintronics functionalities brought about by graphene (and other 2D materials) beyond strengthened PMA, including oxidation protection, atomic thickness control, spin filtering, and spin–orbit torque tailoring.[23–35] Thus, exploring the potential of

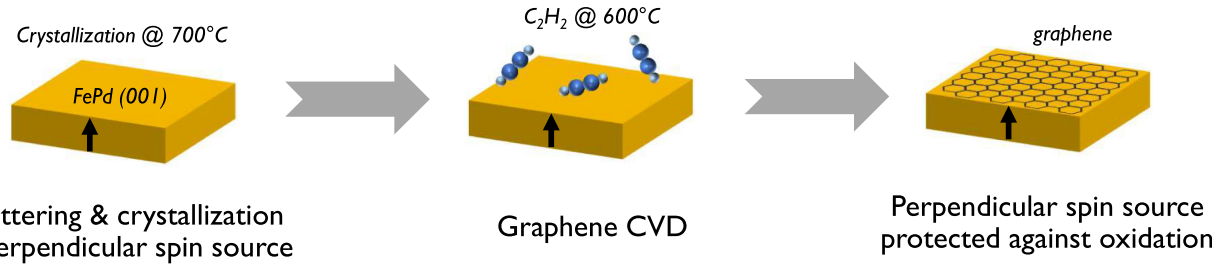

FIG. 1. Schematic illustration of the graphene integration process to the FePd perpendicular spin source. (a) $L1_0$ FePd perpendicular magnetic anisotropy electrode is grown by rf magnetron sputtering at room temperature, followed by an annealing at 700 °C in vacuum.[15–17] (b) The graphene layer is grown by a chemical vapor deposition step.[23,36] (c) This process leads to the fabrication of a perpendicular graphene protected ferromagnetic electrode (GPFE).

hybrid platforms, combining reference perpendicular spin-sources and 2D materials, appears to be very interesting as it may offer advanced opportunities for spintronics. However, this co-integration has proved to be particularly challenging owing to the need for appropriate materials science approaches and developments. As such, even the integration of graphene, the prototypical 2D material, has remained mostly unexplored up until now.

In this Letter, we propose a scheme to integrate large scale graphene with a PMA spintronics platform. The PMA $L1_0$ FePd ordered alloy is grown on $SrTiO_3$ substrates by radio frequency (rf) magnetron sputtering, and consecutively graphene (Gr) is formed on top by a chemical vapor deposition (CVD) step (Fig. 1). The preservation of the FePd crystallographic structure and PMA after graphene deposition is investigated by x-ray diffraction (Fig. 2) and Kerr microscopy (Figs. 3 and 4), respectively. Overall, it appears that our approach allows crystallographic and magnetic properties of the PMA electrode to be robustly preserved during wafer scale integration of CVD graphene. Furthermore, we already demonstrate a potential benefit from graphene integration in this hybrid structure as an x-ray photoemission spectroscopy (XPS) study shows that the Gr/FePd PMA electrode is protected against degradation in oxidative conditions (Fig. 5), showing the achievement of a perpendicular graphene passivated ferromagnetic electrode (GPFE).[23,35] Overall, this work identifies an effective large-scale workflow for the integration of 2D materials with optimized PMA platforms.

The process used for Gr/FePd electrode fabrication is schematically presented in Fig. 1. The FePd layer is deposited on $SrTiO_3$ (0 0 1) substrates by rf magnetron sputtering (EIKO co Ltd; EW-100NH) at room temperature using a $Fe_{40}Pd_{60}$ alloy target. This alloy is specifically designed from molted materials to compensate the different sputtering rates of each element in order to reach a film with the atomic ratio of 50:50 (see Refs. 15–17). The thicknesses of the investigated FePd films are 20 and 30 nm. A reference FePd film is peeled off using diluted *aqua regia* (HNO_3 + 3 HCl). This allows us to analyze its composition using an inductivity coupled plasma optical emission

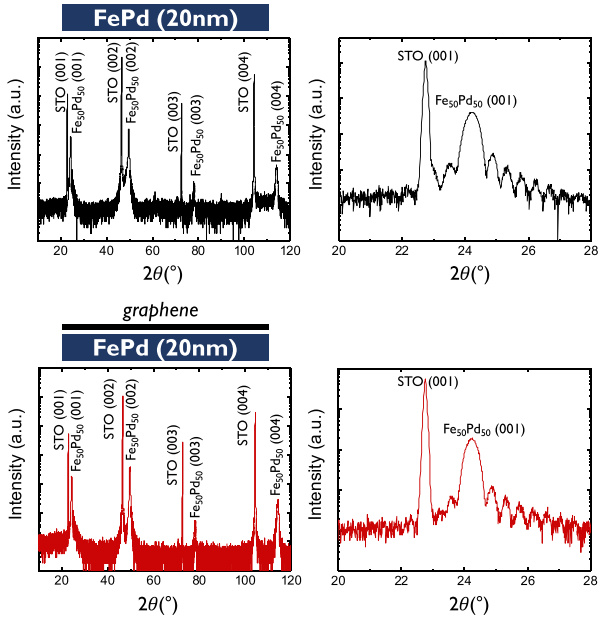

FIG. 2. Out-of-plane x-ray diffraction (XRD) profiles of FePd films before (up) and after (down) graphene growth. Panels on the right show more details of first order peaks with visible Laue oscillations before and after graphene growth. Graphene integration preserves the crystallography of FePd epitaxial films.

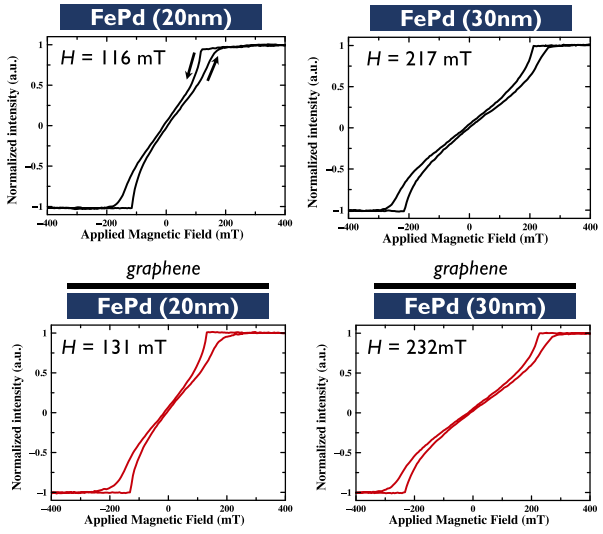

FIG. 3. Polar Kerr hysteresis loops for FePd and Gr/FePd samples are presented in the case of two different FePd thicknesses (20 nm and 30 nm). The magnetization loops are averaged over the entire sample. The PMA domain nucleation field H is given for each case.

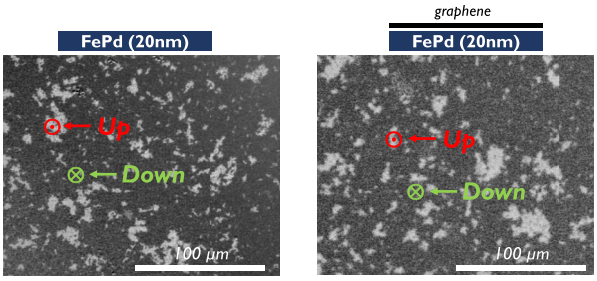

FIG. 4. Polar Kerr images for FePd and Gr/FePd at ∼125 mT after positive magnetic field saturation. Dark areas correspond to uniform magnetization pointing "down" and bright areas to magnetization pointing "up." Similar out-of-plane domains are observed in both the cases. Graphene growth preserves the magnetic properties of FePd as testified by the very similar magnetic textures.

spectrometer (ICP-OES: Seiko SPS4000), showing that it results indeed in a 50:50 FePd alloy. In order to crystallize the films, samples are annealed at 700 °C for 90 min in vacuum by using a substrate heater attached to the sputtering system and then cooled down to room temperature for a few hours in vacuum. The background pressures are 4×10^{-7} Pa before deposition and 5×10^{-5} Pa during annealing at 700 °C. Samples are then transported to a dedicated CVD growth chamber. Reduction and graphene passivation of the FePd surface are achieved by a CVD process (more details of the process used in Refs. 23 and 36) performed in a custom-built cold-wall reactor JCVD system. Samples are heated in a 100 Pa atmosphere of H_2 to 600 °C at 300 °C/min and annealed for 15 min. H_2 is removed, and then the samples are exposed to a 1 Pa atmosphere of C_2H_2 at 600 °C for 15 min. Finally, samples are cooled down in vacuum at ∼100 °C/min. This growth results in a few-layer graphene coating. Previous studies have shown the formation of continuous graphene layers over a large scale by this approach (see, for instance, Ref. 36). Similar Raman and optical studies show the full coverage of graphene on perpendicular

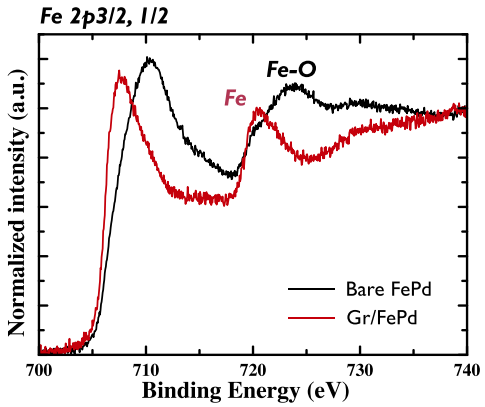

FIG. 5. X-ray photoelectron spectroscopy (XPS) around the binding energy of Fe2p for FePd and Gr/FePd. In contrast to the bare FePd electrode, the FePd surface protected with graphene remains metallic, even after an extended stay in air (no evolution observed during the 1-month study). This result demonstrates the transfer of a specific property of graphene (namely, here its role as a diffusion barrier) to the PMA platform, which is now shown to be compatible with ambient/oxidative processing.

FePd, as further demonstrated below with the XPS results showing full passivation. By combining tailored sputtering[15–17] and CVD[23,36] steps, we are thus able to produce a heterostructure bringing together graphene layers with the perpendicular FePd electrodes.

The interesting properties of the FePd electrode are directly related to its crystallographic order.[17] As the CVD step is based on high temperature annealing in controlled atmospheres, the evolution of the FePd order has to be checked. Hence, in Fig. 2, we show out-of-plane x-ray diffraction (XRD) profiles for FePd on $SrTiO_3$ (0 0 1) substrates before and after graphene deposition. FePd, as grown by sputtering at room temperature, is (1 1 1)-oriented with a polycrystalline structure and transits to the crystalline (0 0 1) structure with the cube-on-cube epitaxial relation after 700 °C annealing, as confirmed by XRD measurements [Figs. 2(a)–2(c)]. The (0 0 1) FePd peak is observed close to 24° as expected for the $L1_0$-FePd 50:50 structure. The large scan XRD measurement shows the presence of only FePd (0 0 1) crystal orientation, with all higher degree peaks. Laue oscillations are clearly visible in Fig. 2(b), showing the high ordering of FePd and confirming the epitaxy of the film. The same measurements are carried out after the growth of CVD graphene [Figs. 2(c) and 2(d)]. Strikingly, we observe that XRD profiles of FePd are unchanged after graphene deposition, thus meaning that the FePd structure is maintained during the CVD process. Laue oscillations are still observed after graphene growth, further assessing the long-distance ordering. This demonstrates that our process of large-scale graphene integration preserves the crystallographic structure of the PMA electrode.

Still, subtle changes in the crystalline order of FePd and additional interaction with graphene overlayer might affect the magnetic properties of this electrode. For this reason, we further explored its perpendicular magnetic behavior through polar Kerr microscopy. In Fig. 3, we present measurements of the perpendicular magnetization (averaged over the entire sample) as a function of the out-of-plane field for FePd and Gr/FePd for two FePd thicknesses of 20 nm and 30 nm. We observe that for both the studied thicknesses, Kerr loops are almost the same for both FePd and Gr/FePd. This confirms that the graphene growth did not substantially modify the PMA properties of FePd films. The magnetization loops show small remanence thanks to the presence of micrometer-size PMA domains (Fig. 4) that lower the dipolar energy of the system. The magnetization saturates above about 200 mT and 300 mT for 20 nm and 30 nm thick films before the Gr deposition, respectively. The magnetic domain nucleation fields are around 100 mT and 200 mT for 20 nm and 30 nm thick FePd films, respectively. Interestingly, we observe that for both FePd thicknesses, a slight increase (about 10%) of both saturation and nucleation fields is measured in the presence of graphene. While this remains to be further studied, this could be ascribed to the interaction of the ferromagnetic electrode with the graphene overlayer. To demonstrate the presence of the magnetic domains, the magnetization of the sample is first saturated by applying an out-of-plane magnetic field of more than 250 mT. Then, the magnetic field is swept down below the nucleation field, until magnetic domains can be observed by polar Kerr microscopy. Images for magnetic fields of about 125 mT are displayed in Fig. 4. A comparable nucleation is observed with and without graphene (the observed nucleation field for the graphene capped sample is 10 mT higher, as expected from the magnetization loop). This observation shows that the perpendicular domain nucleation and propagation mode remain mostly unchanged after the growth of graphene on

top of the FePd electrode. Overall, the integration of graphene is demonstrated to preserve the PMA properties of our FePd platform. The proposed fabrication process, thus, manages to get the definition of a graphene covered magnetic layer with perpendicular magnetization.

Finally, we show that the growth of graphene on FePd protects it from oxidation. We decided to focus on the XPS technique as it is particularly sensitive to the surface (few nm) and allows us to clearly discriminate with high sensitivity the chemical state of the different species, such as Fe, between metallic or oxidized states. XPS analyses thus provide a very strong demonstration of the preservation of the surface state on a large scale (the analyzed spot is $\sim 1\,mm^2$). The XPS spectra at the binding energy of Fe 2p for the FePd and Gr/FePd samples are shown in Fig. 5. In the case of bare FePd, the Fe 2p peak broadens and shifts to higher binding energy due to the presence of FeO ($Fe2p_{2/3} \sim 709\,eV$; $Fe2p_{1/2} \sim 723\,eV$) and/or Fe_2O_3 ($Fe2p_{2/3} \sim 711\,eV$; $Fe2p_{1/2} \sim 724\,eV$). Therefore, the surface of bare FePd appears to be completely oxidized as expected. In contrast, FePd protected with graphene presents only a Fe2p peak with the expected energy splitting of 13.1 eV for the Fe metallic layer. This shows that the CVD step allowed us to recover a metallic FePd surface and to further protect it during exposure to ambient conditions over an extended period. The observed passivation of the FePd surface against oxidation is a further demonstration of the high quality and homogeneity of our graphene coverage thanks to the developed large-scale CVD approach. We checked that no evolution of the Gr/FePd sample occurs over the 1-month study in terms of the crystallographic structure (XRD measurements), magnetism (Kerr measurements), surface morphology (AFM measurements), or surface oxidation (XPS measurements) once left in ambient conditions. This is in stark contrast to the almost immediate oxidation of bare FePd in air. This observation shows the high stabilization provided by graphene coating. It also underlines its strong potential to reduce diffusions and interfacial degradations if integrated in functional heterostructures. We, thus, highlight the benefit of combining 2D materials with PMA layers, as we present here a perpendicular graphene passivated ferromagnetic electrode (GPFE) spin source ready for further integration.[23,35] This result opens the possibility to carry out on top of a high-performance PMA spin platform integrative steps, which are usually forbidden for spintronics, such as oxidative atomic layer deposition (ALD) growth[32] (a conformal process widely used in microelectronics for ultra-thin film deposition[37,38] but barely developed for spintronics) or ambient organics integration.[39] The herein identified hybrid electrode could hence become a PMA reference, unlocking the exploration of systems otherwise difficult to access.

In summary, in this study we show a route to directly integrate graphene layers on top of PMA FePd electrodes via a large-scale CVD approach. Detailed characterization demonstrates that structural and magnetic properties of the PMA electrode are preserved during the graphene CVD growth step. This offers the perspective to combine the performances of PMA and 2D materials for spintronics. Already, we illustrate the benefit of this combination by showing that the FePd electrode, which is naturally degraded by exposition to air, remains robust to oxidation once protected with the graphene layer. We expect this hybrid platform to be a starting point for future investigations of PMA and 2D materials. Many properties remain to be uncovered in these hybrid systems as offered by 2D material-based heterostructures (atomic thickness control, spin filtering, spin–orbit torque modulation…). Further potential is anticipated with the development of large-scale CVD growth of 2D materials on top of PMA electrodes and their integration, for instance, in perpendicular-MTJ devices or in spin-orbitronic systems including schemes based on topological skyrmion spin textures. This exploration will certainly include, in particular, materials such as the 2D insulator h-BN[29,40] and the flourishing family of 2D semiconducting chalcogenides.[41–44]

This work was partly supported by the JSPS core to core program, A. Advanced Research Networks. We acknowledge financial support from the European Commission through the H2020 Future and Emerging Technologies Graphene Flagship (Grant Nos. 881603 and 785219) and Skytop (Grant No. 824123). This research was supported by a public grant overseen by the French National Research Agency (ANR) through FLAG-ERA SographMEM Project Grant No. ANR-19-GRFI-0001-07 and as part of the "Investissements d'Avenir" program (Labex NanoSaclay, Reference: ANR-10-LABX-0035). This study was supported by the JST Program on Open Innovation Platform with Enterprises, Research Institute and Academia (OPERA), KAKENHI (No. 15H03548), Center for Spintronics Integrated Systems (No. J190001511) foundation, and The Murata Science Foundation (072).

REFERENCES

[1]C. Chappert, A. Fert, and F. N. Van Dau, Nat. Mater. **6**, 813 (2007).
[2]A. V. Khvalkovskiy, D. Apalkov, S. Watts, R. Chepulskii, R. S. Beach, A. Ong, X. Tang, A. Driskill-Smith, W. H. Butler, P. B. Visscher, D. Lottis, E. Chen, V. Nikitin, and M. Krounbi, J. Phys. D: Appl. Phys. **46**, 139601 (2013).
[3]T. Endoh, H. Koike, S. Ikeda, T. Hanyu, and H. Ohno, IEEE J. Emerging Sel. Top. Circuits Syst. **6**, 109 (2016).
[4]B. Behin-Aein, D. Datta, S. Salahuddin, and S. Datta, Nat. Nanotechnol. **5**, 266 (2010).
[5]S. Manipatruni, D. E. Nikonov, C.-C. Lin, T. A. Gosavi, H. Liu, B. Prasad, Y.-L. Huang, E. Bonturim, R. Ramesh, and I. A. Young, Nature **565**, 35 (2019).
[6]A. Fukushima, T. Seki, K. Yakushiji, H. Kubota, H. Imamura, S. Yuasa, and K. Ando, Appl. Phys. Exp. **7**, 083001 (2014).
[7]A. Mizrahi, T. Hirtzlin, A. Fukushima, H. Kubota, S. Yuasa, J. Grollier, and D. Querlioz, Nat. Commun. **9**, 1533 (2018).
[8]W. A. Borders, A. Z. Pervaiz, S. Fukami, K. Y. Camsari, H. Ohno, and S. Datta, Nature **573**, 390 (2019).
[9]J. Torrejon, M. Riou, F. A. Araujo, S. Tsunegi, G. Khalsa, D. Querlioz, P. Bortolotti, V. Cros, K. Yakushiji, A. Fukushima, H. Kubota, S. Yuasa, M. D. Stiles, and J. Grollier, Nature **547**, 428 (2017).
[10]V. Cerletti, W. A. Coish, O. Gywat, and D. Loss, Nanotechnology **16**, R27 (2005).
[11]D. D. Awschalom, L. C. Bassett, A. S. Dzurak, E. L. Hu, and J. R. Petta, Science **339**, 1174 (2013).
[12]H. Ohno, T. Endoh, T. Hanyu, N. Kasai, and S. Ikeda, in International Electron Device Meeting-Technical Digest (2010), p. 218.
[13]T. Hanyu, T. Endoh, D. Suzuki, H. Koike, Y. Ma, N. Onizawa, M. Natsui, S. Ikeda, and H. Ohno, Proc. IEEE **104**, 1844 (2016).
[14]D. Houssameddine, U. Ebels, B. Delaët, B. Romacq, I. Firasrau, F. Ponthenier, M. Brunet, C. Thirion, J.-P. Michel, L. Prejbeanu-Buda, M.-C. Cyrille, O. Redon, and B. Dieny, Nat. Mater. **6**, 447 (2007).
[15]H. Naganuma, G. Kim, Y. Kawada, N. Inami, K. Hatakeyama, S. Iihama, K. M. N. Islam, M. Oogane, S. Mizukami, and Y. Ando, Nano Lett. **15**, 623 (2015).
[16]S. Mizukami, F. Wu, A. Sakuma, J. Walowski, D. Watanabe, T. Kubota, X. Zhang, H. Naganuma, M. Oogane, Y. Ando, and T. Miyazaki, Phys. Rev. Lett. **106**, 117201 (2011).
[17]S. Iihama, A. Sakuma, H. Naganuma, M. Oogane, S. Mizukami, and Y. Ando, Phys. Rev. B **94**, 174425 (2016).

[18]H. Yang, A. D. Vu, A. Hallal, N. Rougemaille, J. Coraux, G. Chen, A. K. Schmid, and M. Chshiev, Nano Lett. **16**, 145 (2016).
[19]S. Ikeda, K. Miura, H. Yamamoto, K. Mizunuma, H. D. Gan, M. Endo, S. Kanai, J. Hayakawa, F. Matsukura, and H. Ohno, Nat. Mater. **9**, 721 (2010).
[20]R. Shimabukuro, K. Nakamura, T. Akiyama, and T. Ito, Physica E **42**, 1014 (2010).
[21]H. Yang, M. Chshiev, B. Dieny, J. H. Lee, A. Manchon, and K. H. Shin, Phys. Rev. B **84**, 054401 (2011).
[22]H. Yang, G. Chen, A. A. C. Cotta, A. T. N'Diaye, S. A. Nikolaev, E. A. Soares, W. A. A. Macedo, A. K. Schmid, A. Fert, and M. Chshiev, Nat. Mater. **17**, 605 (2018).
[23]B. Dlubak, M.-B. Martin, R. S. Weatherup, H. Yang, C. Deranlot, R. Blume, R. Schloegl, A. Fert, A. Anane, S. Hofmann, P. Seneor, and J. Robertson, ACS Nano **6**, 10930 (2012).
[24]J.-J. Chen, J. Meng, Y.-B. Zhou, H.-C. Wu, Y.-Q. Bie, Z.-M. Liao, and D.-P. Yu, Nat. Commun. **4**, 1921 (2013).
[25]V. M. Karpan, G. Giovannetti, P. A. Khomyakov, M. Talanana, A. A. Starikov, M. Zwierzycki, J. van den Brink, G. Brocks, and P. J. Kelly, Phys. Rev. Lett. **99**, 176602 (2007).
[26]N. Zibouche, A. Kuc, J. Musfeldt, and T. Heine, Ann. Phys. **526**, 395 (2014).
[27]C. K. Safeer, J. Ingla-Aynés, F. Herling, J. H. Garcia, M. Vila, N. Ontoso, M. R. Calvo, S. Roche, L. E. Hueso, and F. Casanova, Nano Lett. **19**, 1074 (2019).
[28]E. D. Cobas, O. M. J. van't Erve, S.-F. Cheng, J. C. Culbertson, G. G. Jernigan, K. Bussman, and B. T. Jonker, ACS Nano **10**, 10357 (2016).
[29]M. Piquemal-Banci, R. Galceran, M.-B. Martin, F. Godel, A. Anane, F. Petroff, B. Dlubak, and P. Seneor, J. Phys. D: Appl. Phys. **50**, 203002 (2017).
[30]A. Manchon, H. C. Koo, J. Nitta, S. M. Frolov, and R. A. Duine, Nat. Mater. **14**, 871 (2015).
[31]T. Jolicoeur and B. Pandey, Phys. Rev. B. **100**, 115422 (2019).
[32]M.-B. Martin, B. Dlubak, R. S. Weatherup, M. Piquemal-Banci, H. Yang, R. Blume, R. Schloegl, S. Collin, F. Petroff, S. Hofmann, J. Robertson, A. Anane, A. Fert, and P. Seneor, Appl. Phys. Lett. **107**, 012408 (2015).
[33]M. Piquemal-Banci, R. Galceran, F. Godel, S. Caneva, M.-B. Martin, R. S. Weatherup, P. R. Kidambi, K. Bouzehouane, S. Xavier, A. Anane, F. Petroff, A. Fert, S. M.-M. Dubois, J.-C. Charlier, J. Robertson, S. Hofmann, B. Dlubak, and P. Seneor, ACS Nano **12**, 4712 (2018).
[34]W. Lv, Z. Jia, B. Wang, Y. Lu, X. Luo, B. Zhang, Z. Zeng, and Z. Liu, ACS Appl. Mater. Interfaces **10**, 2843 (2018).
[35]F. Godel, M. V. Kamalakar, B. Doudin, Y. Henry, D. Halley, and J.-F. Dayen, Appl. Phys. Lett. **105**, 152407 (2014).
[36]R. S. Weatherup, B. Dlubak, and S. Hofmann, ACS Nano **6**, 9996 (2012).
[37]K. Mistry, C. Allen, C. Auth, B. Beattie, D. Bergstrom, M. Bost, M. Brazier, M. Buehler, A. Cappellani, R. Chau, C.-H. Choi, G. Ding, K. Fischer, T. Ghani, R. Grover, W. Han, D. Hanken, M. Hattendorf, J. He, J. Hicks, R. Heussner, D. Ingerly, P. Jain, R. James, L. Jong, S. Joshi, C. Kenyon, K. Kuhn, K. Lee, H. Liu, J. Maiz, B. McIntyre, P. Moon, J. Neirynck, S. Pae, C. Parker, D. Parsons, C. Prasad, L. Pipes, M. Prince, P. Ranade, T. Reynolds, J. Sandford, L. Shifren, J. Sebastian, J. Seiple, D. Simon, S. Sivakumar, P. Smith, C. Thomas, T. Troeger, P. Vandervoorn, S. Williams, and K. Zawadzki, in IEEE International Electron Devices Meeting (2007), p. 247.
[38]R. W. Johnson, A. Hultqvist, and S. F. Bent, Mater. Today **17**, 236 (2014).
[39]M. Galbiati, S. Tatay, C. Barraud, A. V. Dediu, F. Petroff, R. Mattana, and P. Seneor, MRS Bull. **39**, 602 (2014).
[40]S. Caneva, R. S. Weatherup, B. C. Bayer, B. Brennan, S. J. Spencer, K. Mingard, A. Cabrero-Vilatela, C. Baehtz, A. J. Pollard, and S. Hofmann, Nano Lett. **15**, 1867 (2015).
[41]F. Reale, P. Palczynski, I. Amit, G. F. Jones, J. D. Mehew, A. Bacon, N. Ni, P. C. Sherrell, S. Agnoli, M. F. Craciun, S. Russo, and C. Mattevi, Sci. Rep. **7**, 14911 (2017).
[42]J. Zhou, J. Lin, X. Huang, Y. Zhou, Y. Chen, J. Xia, H. Wang, Y. Xie, H. Yu, J. Lei, D. Wu, F. Liu, Q. Fu, Q. Zeng, C.-H. Hsu, C. Yang, L. Lu, T. Yu, Z. Shen, H. Lin, B. I. Yakobson, Q. Liu, K. Suenaga, G. Liu, and Z. Liu, Nature **556**, 355 (2018).
[43]A. Dankert, P. Pashaei, M. V. Kamalakar, A. P. S. Gaur, S. Sahoo, I. Rungger, A. Narayan, K. Dolui, A. Hoque, M. P. de Jong, R. S. Katiyar, S. Sanvito, and S. P. Dash, ACS Nano **11**, 6389 (2017).
[44]V. Zatko, M. Galbiati, S. M.-M. Dubois, M. Och, P. Palczynski, C. Mattevi, P. Brus, O. Bezencenet, M.-B. Martin, B. Servet, J.-C. Charlier, F. Godel, A. Vecchiola, K. Bouzehouane, S. Collin, F. Petroff, B. Dlubak, and P. Seneor, ACS Nano **13**, 14468 (2019).